

The potential effects of clinical antidiabetic agents on SARS-CoV-2

Hua Qu¹ | Yi Zheng¹ | Yuren Wang^{1,2} | Hongwei Li² | Xiufei Liu¹ |
Xin Xiong¹ | Linlin Zhang¹ | Jing Gu² | Gangyi Yang³ | Zhiming Zhu⁴ |
Hongting Zheng¹  | Qin Ouyang²

¹Department of Endocrinology, Translational Research of Diabetes Key Laboratory of Chongqing Education Commission of China, The Second Affiliated Hospital of Army Medical University, Chongqing, China

²Department of Medicinal Chemistry, College of Pharmacy, Army Medical University, Chongqing, China

³Department of Endocrinology, The Second Affiliated Hospital, Chongqing Medical University, Chongqing, China

⁴Department of Hypertension and Endocrinology, The Third Affiliated Hospital of Army Medical University, Chongqing, China

Correspondence

Hongting Zheng, Department of Endocrinology, Translational Research of Diabetes Key Laboratory of Chongqing Education Commission of China, the Second Affiliated Hospital of Army Medical University, Chongqing, 400037, China.
Email: fnf7703@hotmail.com

Qin Ouyang, Department of Medicinal Chemistry, College of Pharmacy, Army Medical University, Chongqing, China, 400038, China.
Email: ouyangq@tmmu.edu.cn

Funding information

The National Science Fund for Distinguished Young Scholars, Grant/Award Number: 81925007; the National

Abstract

Background: Coronavirus disease 2019 (COVID-19), caused by severe acute respiratory syndrome coronavirus-2 (SARS-CoV-2), is currently posing significant threats to public health worldwide. It is notable that a substantial proportion of patients with severe COVID-19 have coexisting diabetic conditions, indicating the progression and outcome of COVID-19 may relate to diabetes. However, it is still unclear whether diabetic treatment principles can be used for the treatment of COVID-19.

Methods: We conducted a computational approach to screen all commonly used clinical oral hypoglycemic drugs to identify the potential inhibitors for the main protease (M^{PRO}) of SARS-CoV-2, which is one of the key drug targets for anti-COVID-19 drug discovery.

Results: Six antidiabetic drugs with docking scores higher than 8.0 (cutoff value), including repaglinide, canagliflozin, glipizide, gliquidone, glimepiride, and linagliptin, were predicted as the promising inhibitors of M^{PRO}. Interestingly, repaglinide, one of the six antidiabetic drugs with the highest docking score for M^{PRO}, was similar to a previously predicted active molecule nelfinavir, which is a potential anti-HIV and anti-COVID-19 drug. Moreover, we found repaglinide shared similar docking pose and pharmacophores with a reported ligand (N3 inhibitor) and nelfinavir, demonstrating that repaglinide would interact with M^{PRO} in a similar way.

Conclusion: These results indicated that these six antidiabetic drugs may have an extra effect on the treatment of COVID-19, although further studies are necessary to confirm these findings.

KEYWORDS

antidiabetic agents, COVID-19, diabetes, SARS-CoV-2

Hua Qu, Yi Zheng and Yuren Wang contributed equally.

© 2020 Ruijin Hospital, Shanghai Jiaotong University School of Medicine and John Wiley & Sons Australia, Ltd

Key R&D Program of China, Grant/Award Numbers: 2017YFC1309602, 2018YFA0507900, 2016YFC1101100; the National Natural Science Foundation of China, Grant/Award Numbers: 81700714, 81970752, 81471039, 81600673; Talent Project of Third Military Medical University, Grant/Award Numbers: 2017R013, 2019XQYYJ003-2; Special Program for Basic Research Frontier of Military Medicine of the Second Affiliated Hospital of Third Military Medical University, Grant/Award Number: 2018YQYLY006; The Distinguished Young Scholars Training Program of the Third Military Medical University, Grant/Award Number: [2016]609

Highlights

- The progression and outcome of coronavirus disease 2019 (COVID-19) may relate to diabetes; however, whether the diabetic treatment principles can be used for COVID-19 is unclear.
- Here, we screened all commonly used clinical oral hypoglycemic drugs to identify the potential inhibitors of M^{pro} and found six candidate drugs, including repaglinide, canagliflozin, glipizide, gliquidone, glimepiride, and linagliptin.
- The results indicated that these six antidiabetic drugs may have an extra effect on the treatment of COVID-19, although further preclinical experiment and clinical research are necessary to confirm these findings.

1 | INTRODUCTION

Since late December 2019, an epidemic of acute respiratory disease (ARD) in humans started in Wuhan, Hubei Province, China.^{1,2} Further deep sequencing analysis from patient samples revealed a novel coronavirus (CoV), which was named severe acute respiratory syndrome coronavirus-2 (SARS-CoV-2) by the International Committee on Taxonomy of Viruses, and the ARD induced by this CoV was named coronavirus disease 2019 (COVID-19) by the World Health Organization (WHO). To date, more than 881 464 people have been killed by COVID-19, a number that surpasses the toll from SARS in the 2002-03 epidemic worldwide.^{2,3} It was reported that severe COVID-19 cases showed extremely high rates of coexisting diabetes (22.2%-26.9%),^{4,5} and recent study in a cohort of 7337 confirmed COVID-19 cases suggested the progression and outcome of COVID-19 may relate to diabetes.⁶ However, the diabetic treatment principles for COVID-19 patients with diabetes are unclear. Although there are various kinds of clinical antidiabetic agents, how to choose these agents wisely for COVID-19 patients with diabetes, that is, the effect of antidiabetic agents on SARS-CoV-2, remains unknown.

The replication and transcription of CoVs are regulated by the nonstructural proteins (nsps).^{7,8} The 16 mature nsps (nsp1 to 16) are processed from polyproteins (pp1a/1ab) by 2 viral-encoded proteases, including the main protease (M^{pro}) or chymotrypsin-like protease (3CL^{pro}) and papain-like protease (PLPs).^{7,9} Between these 2 proteases, M^{pro} plays a predominant role, and it shares significant homology in amino acid sequence and three-dimensional architecture from human to animal CoVs.^{10,11} Therefore, M^{pro} attracted more attention as a candidate target for the development of drugs to treat CoVs. By targeting M^{pro} it may be possible to develop an anti SARS-CoV-2 inhibitor,¹⁰⁻¹²

which is similar to an anti-HIV drug, nelfinavir, predicted to be a potential inhibitor of SARS-CoV-2 by computational approaches targeting M^{pro} .

Here, we conducted a computational approach to screen all commonly used clinical oral antidiabetic drugs to analyze whether these drugs have a potential inhibition role for M^{pro} of SARS-CoV-2, basing on M^{pro} binding pocket of key residues generated for molecular dynamic simulation.

2 | METHODS

2.1 | Preparation of protein crystal structures

Crystal structure of SARS-CoV-2 M^{pro} was retrieved from RCSB Protein Data Bank (PDB ID: 6 LU7), which was recently reported by Yang et al.¹³ The crystal structure of the complex of M^{pro} with noncovalent ligand X77 was also retrieved (PDB ID: 6W63).¹⁴ The structure was prepared by SYBYL-X 2.0 (Tripos Associates, St. Louis, MO, USA), following methods reported previously.^{15,16} pKa values were calculated using the PDB2PQR Server.^{15,16}

2.2 | Molecular dynamics simulation

Molecular dynamics (MD) simulations were conducted by using AMBER14, gaff force field for small molecules and with ff14SB force field for protein.^{15,16,17} The structures were prepared as previously reported. The N3 inhibitor was bonded with the S atom of CYS145. The MD simulations were carried out under periodic boundary conditions by using NPT ensemble at 300 K after proper minimization and equilibration, according to methods reported previously.¹⁷

2.3 | Trajectory analysis

The trajectory analysis was performed using Amber 14, *cpptraj* module.¹⁸ The root-mean-square deviation (RMSD) was evaluated and equilibrium of the system was assessed by the RMSD values. The average structures of models were calculated based on the equilibrium time in MD simulation, using the *cpptraj* module.

2.4 | Calculation of binding free energies

The binding free energies of proteins to ligands were calculated when reached equilibrium state in aforementioned MD simulation, using the molecular mechanics generalized Born surface area (MM/GBSA) method¹⁹ implemented in Amber 14. Protocols and parameters were reported previously.¹⁹ Based on the calculated binding free energies, the key residues employing more contribution to the binding interaction would be identified.

2.5 | Molecular docking study

The crystal structures of SARS-CoV-2 main protease was extracted from its complex by using an inhibitor N3 (PDB ID: 6LU7). Docking studies were performed using Surflex-Dock in SYBYL-X 2.0 software with Surflex-Dock Geomx (SFXC) mode. The pre-dock minimization, post-dock minimization, consider ring flexibility, molecule fragmentation, and the soft grid treatment were set as on. Based on the key residues with default setting (Threshold 0.5 and Bloat 0), the binding pocket was generated. The key residues for SARS-CoV-2 main protease included LEU27, HIS41, MET49, CYS145, MET165, GLU166, PRO168, ASP187, and GLN189. The docked complex with the highest score was chosen for the molecular dynamic simulation.²⁰ The binding free energies were calculated by MM/GBSA method. The interactions of binding between the M^{Por} and ligands were determined using LigPlot+.^{21,22}

2.6 | Cell culture and reagents

Human alveolar type II cells (A549) were cultured in DMEM (Gibco) with 10% fetal bovine serum (FBS) and human umbilical vein endothelial cells (HUVECs) were cultured in 1640 medium (Gibco) with 10% FBS according to the recommendation from the suppliers. Cell identities and mycoplasma determinations were done by Shanghai Biowing Biotechnology Co. Commercial antidiabetic drugs for humans including repaglinide (Novo Nordisk), canagliflozin (Janssen Pharmaceuticals), glipizide (Zibo

Wanjie Pharmaceutical), gliquidone (Beijing Wanhui Shuanghe Pharmaceutical), glimepiride (Sanofi Aventis), and linagliptin (Boehringer Ingelheim Pharmaceuticals) from the listed companies were also used.

2.7 | Quantitative real-time polymerase chain reaction (qRT-PCR)

qRT-PCR analyses were performed as previously described.²³ In brief, by using Trizol (Takara), total RNA of cells was isolated according to the instructions, and then 1 µg of total RNA was reverse transcribed to cDNA by PrimeScript Reagent Kit (Takara). The PCR amplification was performed using SYBR Green (Takara). Expression levels of mRNA were calculated by the Δ Ct-method. The following primer pairs were used in this study: angiotensin-converting enzyme 2 (ACE2): forward 5'-GAGGAAAAGGCCGAGAGCTT-3', and reverse 5'-GACGCTTGATGGTCGCATTC-3'; L-SIGN: forward 5'-CTCCTGGGGTGTCTTGGC-3', and reverse 5'-GTCCAGTCCTTGGGACAGTG-3'; DC-SIGN: forward 5'-GCAAGACGCGATCTACCAGA-3', and reverse 5'-CCAGGGGAAATTGGAGGCAT-3'.

2.8 | Western blot

Cells were treated as indicated and were collected in lysis buffer and prepared as previously described.²³ The concentrations of protein in each cell lysate were analyzed by the Protein Assay Kit (BCA assay). Then, proteins in the lysates were separated by SDS-PAGE and immune-blotted with the ACE2 primary antibodies (1:1000, proteintech) and its corresponding secondary antibodies. Images were acquired using fusion FX5s system (Vilber Lourmat).²³

2.9 | Statistical analysis

All data were analyzed by the GraphPad Prism 7.0 (Macintosh). Quantitative values were presented as the mean \pm SEM. For multiple comparison analysis, one-way analysis of variance with Tukey's multiple comparison tests was used. *P* values <0.05 were considered to be statistically significant.

3 | RESULTS

3.1 | Molecular dynamics study to explore the binding pocket of M^{Por}

We first conducted a molecular dynamics simulation for 200 ns to determine the key residues in the binding

pocket of M^{PPO} and investigated the stability of the M^{PPO} /N3 inhibitor complex by monitoring the RMSD. The N3 inhibitor was connected with M^{PPO} by C-S covalent bond. After molecular dynamics, the N-terminus residues of M^{PPO} (near the binding interface) showed slight fluctuation, and the loop at the C-terminus showed greater variation (Figure 1A). M^{PPO} attained its equilibrium (plateau) state at 50 ns, with the RMSD value of 2.70 Å (Figure 1B), whereas the values for the N3 inhibitor were 10 ns, and 1.84 Å (Figure 1B). Because of the covalent bond, the conformation of the ligand was slightly shaking.

To assess the interactions between these two systems, the hydrogen bond analyses were carried out based on the MD simulation. In the crystal structure of M^{PPO} and N3, seven residues, including THR190, GLN189, HIS164, GLU166, HIS163, PHE140, and GLY143, to form N3 hydrogen bonds (Figure S1). During the MD simulation, the hydrogen bonds between GLN189, HIS164, GLU166, THR24, HIS41, and GLU143 with N3 were found in more

than 10% of the frames of the MD trajectory. To calculate the contribution of each residue, the MM/GBSA free energy and the decomposition energy M^{PPO} /N3 system were calculated (Figure 1C), which suggested that GLN189, MET165, MET49, and PRO168 contributed favorable energies lower than -2.0 kcal/mol. Among these residues, there are hydrogen bonds between GLN189 and N3, whereas the binding interaction between MET165, MET49, PRO168, and N3 was hydrophobic interaction from the side chain of M^{PPO} and N3. Other residues, including GLU166 and HIS41, also proved important to the interaction of hydrogen bonds with energy contributions lower than -0.8 kcal/mol, and LEU27, CYS145, and ALA191 was binding with ligand by hydrophobic interaction.

To further confirm the residues for the binding pocket, 200 ns dynamics simulation and corresponding MM/GBSA free energy were also carried out for the complex of M^{PPO} with noncovalent ligand X77 (Figure S2). The total energy in M^{PPO} -X77 system was

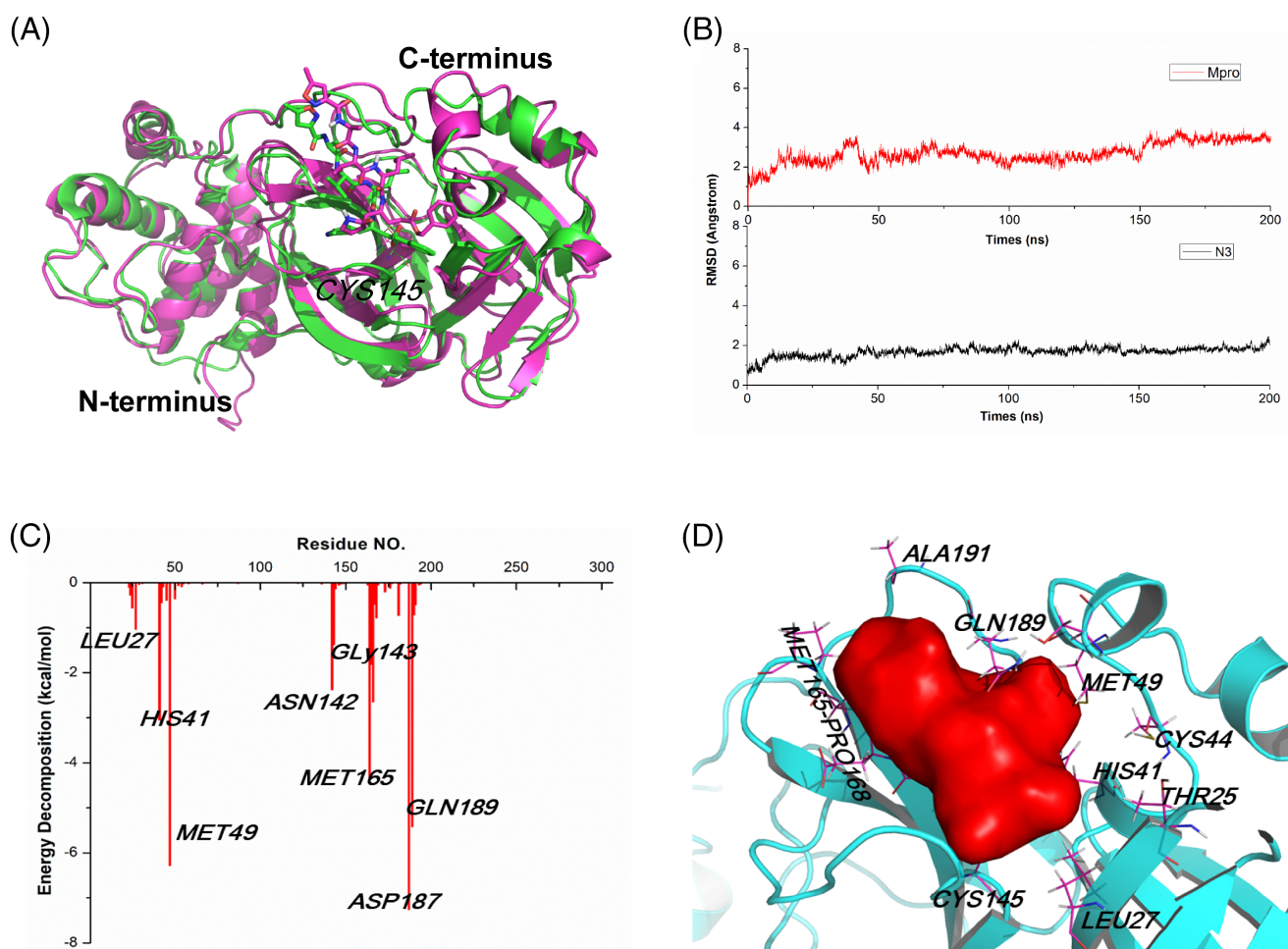


FIGURE 1 Molecular dynamics study to explore the binding pocket of M^{PPO} . A, The crystal structure superimposed on the last configuration after 200 ns of simulation for M^{PPO} and N3 inhibitor. The initial and the last configurations were shown in green and magenta, respectively. B, The root-mean-square deviation (RMSD) of M^{PPO} and N3 inhibitor. C, Binding free energy decomposition of M^{PPO} and N3 inhibitor system. D, The key residues for the binding interaction of M^{PPO} and N3 inhibitor and the binding pocket of M^{PPO}

-30.58 ± 4.29 kcal/mol, resulting from Van der Waals (VDW) energy (ΔE_{vdw}), electrostatic energy ($\Delta E_{\text{electrostatic}}$), electrostatic contribution solvation free energy (ΔG_{GB}), and nonpolar solvation free energy (ΔG_{SA}) with the values of -41.74 ± 5.07 , -12.26 ± 4.28 , 28.74 ± 4.46 , and -5.33 ± 0.51 kcal/mol, respectively (Table S1). Obviously, ΔE_{vdw} terms made the greatest contribution to this binding, indicating that VDW interactions generated the primary binding energy in the system. As initial structure, in the crystal structure, there are three hydrogen binding energy between X77 and residues GLU166, HIS163, and GLY143; however, their energy contributions are greater than -0.8 kcal/mol according to the decomposition energy calculation. On the other side, HIS41, MET49, LEU50, CYS145, MET165, ASP187, and GLN189 contributed favorable energies lower than -0.8 kcal/mol. The hydrogen bond analyses suggested there are hydrogen bonds between HIS41, GLU189, and X77. Other residues might interact with X77 by hydrophobic interaction. Based on these residues, we established the binding pocket by SYBYL program (Figure 1D).

3.2 | Prediction of the potential ligands for M^{pro}

Next, we in silico screened all commonly used clinical oral antidiabetic drugs suggested by guideline from the Chinese Diabetes Society²⁴ to predict the potential inhibitors for M^{pro} . Molecular docking was carried out between M^{pro} and 22 different hypoglycemic drugs listed in Table S2. Nelfinavir, a previously predicted active molecule bound to M^{pro} , was selected as the positive control and produced a total docking score of 9.63. After evaluating the interaction by analyses of the docking scores and binding poses, repaglinide, canagliflozin, glimepiride, glipizide, gliquidone, and linagliptin were predicted as the promising chemical agents. Our results showed that these six antidiabetic drugs with docking scores higher than 8.0 (Table S2) shared similar binding poses to the reported ligand N3 inhibitor in the crystal structure (Figure 2). Among these six antidiabetic drugs, repaglinide employed the highest docking score for M^{pro} (9.3). In these binding conformations, we found some hydrogen bonds existing between drugs and HIS164, GLU166, GLY143, and ASP187. The hydrophilic-hydrophobic interactions should also be important for their binding interaction, because the VDW interaction was the primary contribution to the binding of reported ligand N3 inhibitor with M^{pro} . We also compared the binding residues of each ligand with the key residues identified by molecular dynamic simulation of M^{pro} -N3

system and M^{pro} -X77 (Figure S3 and Table S3). We found gliquidone, repaglinide, and glipizide interacted with most of these key residues, which implied that these ligands have more possibility of inhibiting M^{pro} .

3.3 | Analysis of the structure and binding interaction of repaglinide

Based on binding conformations alignment and similarity calculation, we found repaglinide shared similar pharmacophores with nelfinavir and the reported ligand N3 among these six drugs. Repaglinide is an insulinotropic agent, classified as the nonsulfonylurea type, whose mass weight was lower than N3 inhibitor or nelfinavir, whereas their shapes and pharmacophores were similar. The docking model of repaglinide with M^{pro} turned out to be similar with that of the reported ligand (N3 inhibitor) and nelfinavir, where two hydrogen bonds involving GLU166 and HIS164 maintained the binding interface between repaglinide and SARS-CoV-2 M^{pro} . Moreover, repaglinide also shared an analogous docking pose (Figure 3A and B) with N3 inhibitor and nelfinavir, as well as similar pharmacophores including hydrophobic alkyl, hydrophilic ring, aromatic ring, and hydrophobic ring. In particular, repaglinide and N3 inhibitor shared a similar leucine (LEU) analogue structure in their hydrophobic alkyl moiety.

To gain more insights into the binding mechanism, docking complex of repaglinide- M^{pro} were subjected to 50 ns molecular dynamics simulations using Amber 14. The binding free energies were calculated by MM/GBSA approaches. The results showed that (a) the binding free energies of repaglinide- M^{pro} are -28.48 ± 3.27 kcal/mol, similar with the recently reported nelfinavir and X77 inhibitor; (b) VDW interaction (E_{vdw}) makes a more significant contribution than the electrostatic interaction (E_{ele}) (Table S1), indicating that E_{vdw} is the driving force for binding. The energy decomposition in the repaglinide- M^{pro} system was calculated (Figure S4), where GLN192, MET165, ALA191, GLN189, and MET49 contributed favorable energies lower than -1.0 kcal/mol, consistent with the key residues of the binding pocket defined by ligand (N3 and X77 inhibitor). These observations further demonstrated that repaglinide interacted with M^{pro} in a similar way with that of the existing inhibitors.

On the other hand, cell penetration is also a pivotal step during the infection of CoVs. Recent studies found that ACE2 was a possible cellular entry receptor for SARS-CoV-2, because the virus was proved unable to infect cells with absence of ACE2.^{25,26} Therefore, we assessed the effects of these six antidiabetic drugs on ACE2 expression in human alveolar type II cell line A549

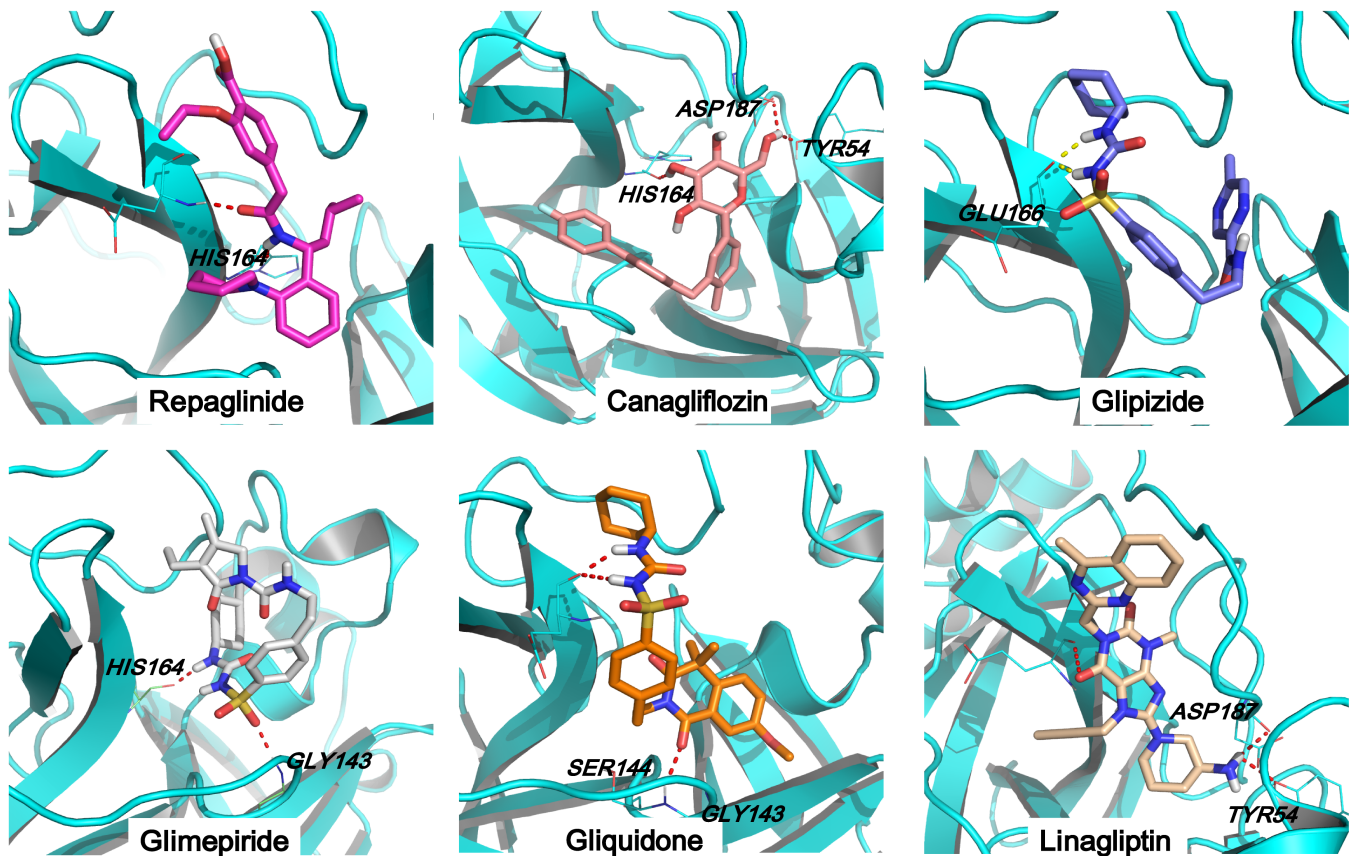


FIGURE 2 Prediction of the potential ligands for M^{pro} . The docking mode of M^{pro} and repaglinide, canagliflozin, glimepiride, glipizide, gliquidone, and linagliptin, respectively

and vascular endothelial cells (HUVEC), which represented the major expression position of ACE2 and showed an upregulated ACE2 expression under carcinogen exposures or inflammation.²⁷⁻³⁰ Our results showed that they had no significant influences on the expressions of ACE2 (Figure 3C and D). In addition to ACE2, other receptors, such as L-SIGN (also known CD209L) and DC-SIGN (also known as CD209), were reported to affect SARS-CoV-2 host entry.³¹ Therefore, we further detected the expression of these two receptors in A549 and HUVEC cells after treated by the selected antidiabetic drugs, and we did not find significant changes at the mRNA expression levels of both L-SIGN and DC-SIGN (Figure S5).

4 | DISCUSSION

In this study, we performed a novel strategy to in silico screen 22 clinical oral antidiabetic drugs and identify six medicines with potential inhibition for M^{pro} of SARS-CoV-2. Interestingly, repaglinide, an anti-HIV drug²⁰ employed the similar pharmacophores, LEU analogical substrate, and M^{pro} docking score to nelfinavir, is predicted as a promising candidate for treatment of COVID-19.

We demonstrated six antidiabetic drugs, including repaglinide, canagliflozin, glipizide, gliquidone, glimepiride, and linagliptin, possessed the ability to bind with M^{pro} binding pocket, indicating they may act to suppress the replication and transcription of SARS-CoV-2. Here we established the receptor-based virtual screening approach for the potential inhibitor of M^{pro} . Compared with the standard assay that was used to test whether the existing hypoglycemic drugs are effective in treating the viral infections,³² our method could quickly and with high throughput screen drugs for repurposing or easily obtained compounds and shorten the time for new drug development.^{33,34}

Through this model, six antidiabetic drugs are predicted as promising inhibitors for M^{pro} , as they gained the docking scores between 8.5 ~ 9.3. In general, a great docking score means more possibility to bind to the target protein with high binding affinity. Here, a relative higher cutoff value of 8.0 was selected to find the more promising candidates. The binding conformations of these antidiabetic drugs with M^{pro} suggested these molecules may inhibit the replication and transcription of CoV, which in accordance with previous studies that lopinavir, a marketed status drug developed by targeting

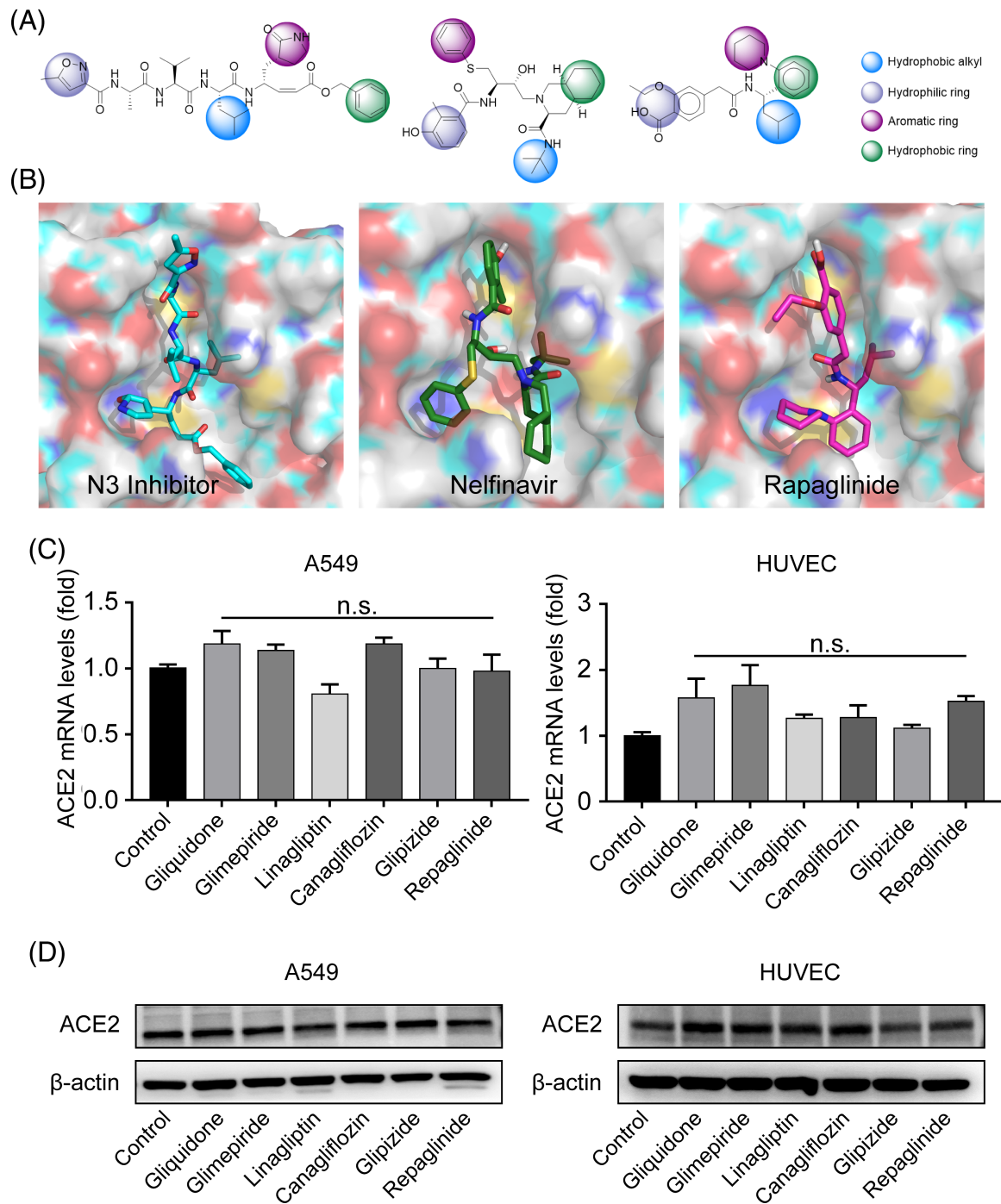


FIGURE 3 The pharmacophores and binding poses with M^{pro}, as well as the effect on angiotensin-converting enzyme 2 (ACE2) expression of indicated drugs. A, The structure and pharmacophores of N3 inhibitor, nelfinavir, and repaglinide. B, The binding conformations of N3 inhibitor (crystal structure), nelfinavir, and repaglinide with the pocket. C and D, A549 and human umbilical vein endothelial cells (HUVEC) cells were treated by repaglinide (2 μM), canagliflozin (50 μM), glimepiride (50 μM), glipizide (50 μM), gliquidone (50 μM), and linagliptin (50 nM) respectively for 2 hours, the mRNA (C) and protein (D) expressions of ACE2 were assessed by quantitative real-time polymerase chain reaction and immunoblotting. n = 3 independent studies for (C) and (D). Data are presented as means ± SEM. n.s., not significant compared with control

M^{pro}, now was found to improve the outcome of Middle East respiratory syndrome (MERS)-CoV infected common marmosets, as well as SARS patients in

nonrandomized trials.^{35,36} We also found lopinavir may bind to the binding pocket of M^{pro} with docking score of 10.04 (Table S2). However, Cao et al³⁷ reported a single-

center and open-label trial that evaluated the therapeutic effects of lopinavir-ritonavir treatment in hospitalized adult patients with severe COVID-19; however, they found no benefit from this treatment compared with standard care. Consistently, another trial conducted in a mild/moderate COVID-19 population also reported a negative result of lopinavir-ritonavir therapy.³⁸ Recently, WHO announced the results of the SOLIDARITY trial, the largest international randomized trial regarding antiviral drugs for COVID-19, and they also found no effect of lopinavir on hospitalized COVID-19.³⁹ These findings remind us to confront the gap between molecular structural information and clinical effectiveness. Thus, the molecular docking results need to be interpreted with caution.

Others also reported the potentially druggable target of M^{Pro} by the molecular docking approach and identify numerous classes of protease inhibitors against SARS-CoV, such as GRL-001.^{10,40,41} More important, our structure analysis showed repaglinide, belonging to the meglitinide class of short-acting insulin secretagogues, employed a similar structure and docking score (9.3) as an anti-HIV drug nelfinavir (9.6), which was recently suggested to be a potential inhibitor against SARS-CoV-2 M^{Pro}.²⁰ In addition, based on binding conformations alignment and similarity calculation of these six drugs with nelfinavir, we found repaglinide shared similar docking pose (Figure 3A and B) and pharmacophores with the reported ligand in the crystal structure of M^{Pro} (N3 inhibitor) and nelfinavir, including hydrophobic alkyl, hydrophilic ring, aromatic ring, and hydrophobic ring. In particular, we identified the similar LEU amino acid substrate as a reported ligand N3 inhibitor shared by repaglinide and nelfinavir, suggesting that LEU analogical fragments might be important for the discovery of new M^{Pro} inhibitors. Although the docking scores and predicted binding affinity of the other five antidiabetic drugs were lower than those of nelfinavir, we may take advantage of these hypoglycemic drugs for the additional benefits of anti-SARS-CoV-2 effects when hypoglycemic treatment is necessary to COVID-19 patients with diabetes mellitus. Notably, although our results indicated that all these six antidiabetic drugs might not affect the expression of ACE2 and other two potential receptors, that is, L-SIGN and DC-SIGN, a recent study also found other influence factors of SARS-CoV-2 host entry, such as cellular serine protease TMPRSS2,⁴² which required to be examined in future studies. Besides M^{Pro}, various factors have been found to affect the infection of SARS-CoV-2, and several drugs including metformin and sitagliptin that were assessed at lower docking scores in our study were reported to show positive outcomes in COVID-19 patients.^{43,44} Therefore, we cannot exclude the possibility that drugs that rank lower in our docking results of M^{Pro} may have a beneficial role in

hindering the replication and infection of SARS-CoV-2 through other ways. In addition, dipeptidyl peptidase 4 (DPP4) has been reported as a receptor for human coronavirus (hCoV-EMC) that directly binds to DPP4 through its S1 domain. Antibodies against DPP4 could inhibit hCoV-EMC infection of primary human bronchial epithelial cells and Huh-7 cells, whereas DPP4-inhibitors including sitagliptin, vildagliptin, and saxagliptin were not able to block the infections.⁴⁵ These findings indicated that the binding interface between the virus and receptor might differ from the developed receptor inhibitors that were designed for lowering blood glucose.

In sum, our results indicated the potential extra effects on anti-SARS-CoV-2 by the six oral antidiabetic drugs. Further preclinical experiment and clinical research are necessary to confirm these findings, and the effects of insulin and GLP1 analogues on SARS-CoV-2 also need to be tested in the future.

ACKNOWLEDGEMENTS

We thank Zihe Rao and Haitao Yang group from Shanghai Institute for Advanced Immunochemical Studies (SIAIS) for the crystal structure of M^{Pro} (PDB ID: 6LU7).

This work was supported by the National Science Fund for Distinguished Young Scholars (No. 81925007), the National Key R&D Program of China (No. 2017YFC1309602, No. 2018YFA0507900 and No. 2016YFC1101100), the National Natural Science Foundation of China (No. 81700714, No. 81970752, No. 81471039 and No. 81600673), “Talent Project” of Third Military Medical University (2017R013 and 2019XQYYYJ003-2), Special Program for Basic Research Frontier of Military Medicine of the Second Affiliated Hospital of Third Military Medical University (2018YQYLY006), and the Distinguished Young Scholars Training Program of the Third Military Medical University (School administration No. [2016]609).

DISCLOSURE

None declared.

ORCID

Hongting Zheng  <https://orcid.org/0000-0002-6930-0103>

REFERENCES

1. Huang C, Wang Y, Li X, et al. Clinical features of patients infected with 2019 novel coronavirus in Wuhan, China. *Lancet (London, England)*. 2020;395:497-506.
2. WHO Coronavirus Disease (COVID-19) Dashboard. 2020. <https://covid19.who.int/>. Accessed September 7, 2020.
3. Summary of Probable SARS Cases with Onset of Illness from 1 November 2002 to 31 July 2003. 2003. https://www.who.int/csr/sars/country/table2004_04_21/en/. Accessed February 10, 2020.

4. W-j G, Z-y N, Hu Y, et al. Clinical characteristics of 2019 novel coronavirus infection in China. *N Engl J Med.* 2020;382:1708-1720.
5. Wang D, Hu B, Hu C, et al. Clinical characteristics of 138 hospitalized patients with 2019 novel coronavirus-infected pneumonia in Wuhan, China. *JAMA.* 2020;323:1061-1069.
6. Zhu L, She ZG, Cheng X, et al. Association of blood glucose control and outcomes in patients with COVID-19 and pre-existing type 2 diabetes. *Cell Metab.* 2020;31:1068-1077. e3.
7. Perlman S, Netland J. Coronaviruses post-SARS: update on replication and pathogenesis. *Nat Rev Microbiol.* 2009;7:439-450.
8. de Wit E, van Doremalen N, Falzarano D, Munster VJ. SARS and MERS: recent insights into emerging coronaviruses. *Nat Rev Microbiol.* 2016;14:523-534.
9. Fehr AR, Perlman S. Coronaviruses: an overview of their replication and pathogenesis. *Methods Mol Biol.* 2015;1282:1-23.
10. Yang H, Xie W, Xue X, et al. Design of wide-spectrum inhibitors targeting coronavirus main proteases. *PLoS Biol.* 2005;3:e324.
11. Xue X, Yu H, Yang H, et al. Structures of two coronavirus main proteases: implications for substrate binding and antiviral drug design. *J Virol.* 2008;82:2515-2527.
12. Anand K, Ziebuhr J, Wadhvani P, Mesters JR, Hilgenfeld R. Coronavirus main proteinase (3CLpro) structure: basis for design of anti-SARS drugs. *Science.* 2003;300:1763-1767.
13. The crystal structure of 2019-nCoV main protease in complex with an inhibitor N3. 2020. <http://www.rcsb.org/structure/6LU7>. Accessed February 12, 2020.
14. Structure of COVID-19 main protease bound to potent broad-spectrum non-covalent inhibitor X77. 2020. <https://www.rcsb.org/structure/6w63>. Accessed September 7, 2020.
15. PDB2PQR Server. 2020. http://nbc-222.ucsd.edu/pdb2pqr_2.0/. Accessed February 10, 2020.
16. Dolinsky TJ, Nielsen JE, McCammon JA, Baker NA. PDB2PQR: an automated pipeline for the setup of Poisson-Boltzmann electrostatics calculations. *Nucleic Acids Res.* 2004;32:W665-W667.
17. Maier JA, Martinez C, Kasavajhala K, Wickstrom L, Hauser KE, Simmerling C. ff14SB: improving the accuracy of protein side chain and backbone parameters from ff99SB. *J Chem Theory Comput.* 2015;11:3696-3713.
18. Roe DR, Cheatham TE 3rd. PTRAJ and CPPTRAJ: software for processing and analysis of molecular dynamics trajectory data. *J Chem Theory Comput.* 2013;9:3084-3095.
19. Hou T, Wang J, Li Y, Wang W. Assessing the performance of the MM/PBSA and MM/GBSA methods. 1. The accuracy of binding free energy calculations based on molecular dynamics simulations. *J Chem Inform Model.* 2011;51:69-82.
20. Xu Z, Peng C, Shi Y, et al. Nelfinavir was predicted to be a potential inhibitor of 2019-nCoV main protease by an integrative approach combining homology modelling, molecular docking and binding free energy calculation. *bioRxiv.* 2020;921627. <https://doi.org/10.1101/2020.01.27.921627>.
21. Laskowski RA, Swindells MB. LigPlot+: multiple ligand-protein interaction diagrams for drug discovery. *J Chem Inf Model.* 2011;51:2778-2786.
22. Suresh PK, Divya N, Nidhi S, Rajasekaran R. Phenytoin-bovine serum albumin interactions - modeling plasma protein - drug binding: a multi-spectroscopy and in silico-based correlation. *Spectrochim Acta A Mol Biomol Spectrosc.* 2018;193:523-527.
23. Zheng Y, Qu H, Xiong X, et al. Deficiency of mitochondrial glycerol 3-phosphate dehydrogenase contributes to hepatic steatosis. *Hepatology.* 2019;70:84-97.
24. Society CD. Guidelines for the prevention and treatment of type 2 diabetes in China (2017 edition). *Chin J Diabetes Mellitus.* 2018;10(1):4-67.
25. Zhou P, Yang XL, Wang XG, et al. A pneumonia outbreak associated with a new coronavirus of probable bat origin. *Nature.* 2020;579:270-273.
26. Jiang RD, Liu MQ, Chen Y, et al. Pathogenesis of SARS-CoV-2 in transgenic mice expressing human angiotensin-converting enzyme 2. *Cell.* 2020;182:50-58.e8.
27. Smith JC, Sausville EL, Girish V, et al. Cigarette smoke exposure and inflammatory signaling increase the expression of the SARS-CoV-2 receptor ACE2 in the respiratory tract. *Dev Cell.* 2020;53:514-529. e3.
28. Hamming I, Timens W, Bulthuis ML, Lely AT, Navis G, van Goor H. Tissue distribution of ACE2 protein, the functional receptor for SARS coronavirus. A first step in understanding SARS pathogenesis. *J Pathol.* 2004;203:631-637.
29. Choi JY, Lee HK, Park JH, et al. Altered COVID-19 receptor ACE2 expression in a higher risk group for cerebrovascular disease and ischemic stroke. *Biochem Biophys Res Commun.* 2020;528:413-419.
30. Mompeon A, Lazaro-Franco M, Bueno-Beti C, et al. Estradiol, acting through ERalpha, induces endothelial non-classic renin-angiotensin system increasing angiotensin 1-7 production. *Mol Cell Endocrinol.* 2016;422:1-8.
31. Amraie R, Napoleon MA, Yin W, et al. CD209L/SIGN and CD209/DC-SIGN act as receptors for SARS-CoV-2 and are differentially expressed in lung and kidney epithelial and endothelial cells. *bioRxiv.* 2020;165803.
32. Wang M, Cao R, Zhang L, et al. Remdesivir and chloroquine effectively inhibit the recently emerged novel coronavirus (2019-nCoV) in vitro. *Cell Res.* 2020;30:269-271.
33. Uba AI, Yelekcı K. Identification of potential isoform-selective histone deacetylase inhibitors for cancer therapy: a combined approach of structure-based virtual screening, ADMET prediction and molecular dynamics simulation assay. *J Biomol Struct Dyn.* 2018;36:3231-3245.
34. Lu H, Stratton CW, Tang YW. Outbreak of pneumonia of unknown etiology in Wuhan, China: the mystery and the miracle. *J Med Virol.* 2020;92:401-402.
35. Chan K, Lai S, Chu C, et al. Treatment of severe acute respiratory syndrome with lopinavir/ritonavir: a multicentre retrospective matched cohort study. *Hong Kong Med J.* 2003;9:399-406.
36. Chu MC. Role of lopinavir/ritonavir in the treatment of SARS: initial virological and clinical findings. *Thorax.* 2004;59:252-256.
37. Cao B, Wang Y, Wen D, et al. A trial of lopinavir-ritonavir in adults hospitalized with severe COVID-19. *N Engl J Med.* 2020;382:1787-1799.
38. Li Y, Xie Z, Lin W, et al. Efficacy and safety of Lopinavir/ritonavir or arbidol in adult patients with mild/moderate COVID-19: an exploratory randomized controlled trial. *Med (N Y).* 2020.
39. Pan H, Peto R, Karim QA, et al. Repurposed antiviral drugs for COVID-19 –interim WHO SOLIDARITY trial results. *medRxiv.* 2020;20209817.

40. Adedeji AO, Sarafianos SG. Antiviral drugs specific for coronaviruses in preclinical development. *Curr Opin Virol.* 2014;8:45-53.
41. Ren Z, Yan L, Ning Z, et al. The newly emerged SARS-like coronavirus HCoV-EMC also has an "Achilles' heel": current effective inhibitor targeting a 3c-like protease. *Protein Cell.* 2013;4:248-250.
42. Hoffmann M, Kleine-Weber H, Schroeder S, et al. SARS-CoV-2 cell entry depends on ACE2 and TMPRSS2 and is blocked by a clinically proven protease inhibitor. *Cell.* 2020;181:271-280. e8.
43. Hariyanto TI, Kurniawan A. Metformin use is associated with reduced mortality rate from coronavirus disease 2019 (COVID-19) infection. *Obes Med.* 2020;19:100290.
44. Solerte SB, D'Addio F, Trevisan R, et al. Sitagliptin treatment at the time of hospitalization was associated with reduced mortality in patients with type 2 diabetes and COVID-19: a multicenter, case-control, retrospective, observational study. *Diabetes Care.* 2020;dc201521. <https://doi.org/10.2337/dc20-1521>.
45. Raj VS, Mou H, Smits SL, et al. Dipeptidyl peptidase 4 is a functional receptor for the emerging human coronavirus-EMC. *Nature.* 2013;495:251-254.

SUPPORTING INFORMATION

Additional supporting information may be found online in the Supporting Information section at the end of this article.

How to cite this article: Qu H, Zheng Y, Wang Y, et al. The potential effects of clinical antidiabetic agents on SARS-CoV-2. *Journal of Diabetes.* 2021;13:243–252. <https://doi.org/10.1111/1753-0407.13135>